A Morphological Approach to the Aeroacoustic Fields of a Flute with Density Gradient Correlation

Yasuo Obikane, Florent Margnat

20th AIAA Computational Fluid Dynamics Conference
27 - 30 June 2011, Honolulu, Hawaii

AIAA 2011-3683

A Morphological Approach to the Aero-acoustic Fields of a Flute with Density Gradient Correlation

Yasuo Obikane[1]
Sophia University, Mech. Eng., 7-1 Kioi-chou Chiyoda-ku Tokyo, 102-8554, Japan

and

Florent Margnat[2]
Arts et Metiers ParisTech, DynFluid, 151 bd de l'Hopital, 75013 Paris ,France

Sound generations from Ocarina, an Italian musical instrument, are simulated and the density gradient correlations of the flow fields are studied. We successfully generated the sound radiated from the Ocarina with fully open sides and also with one hole in each side of the body. The meshes are taken 100x60x100 (coarse) and 200x120x200 (finer). We compare the pressure patterns to the second and third invariants of the density gradient correlation. This methodology is also applied to the sound radiated by a subsonic mixing-layer, as a comparison. For both flows, it is found that the invariant variables can better extract the characteristics of the fields. The invariant pictures can show the movement of the contraction and expansion of the density well. The results imply that both the fluctuating density gradient correlation and the invariants can be a good index to show the compressibility in low speed aero-acoustics. In addition, the patterns of the invariants are clearer in the finer computations.

Nomenclature

ρ	=	density
$,i$	=	spatial derivative with respect to i-th direction
m_i	=	ρu_i
u_i	=	Cartesian velocity of i-th direction
$\overline{\rho_{,p}\rho_{,q}}$	=	density gradient correlation in p , q direction
ε	=	the total energy
p	=	static pressure
μ	=	viscosity
P_r	=	Prandtl number

I. Introduction

RESEARCH on members of the flute family like the recorder, the long flute, and the ocarina have mainly concentrated on propagation, reflection, attenuation, and impedance of sound, but ignored how the sound is generated in aero-acoustics. Previous studies[4] used the sound generated by some mechanical variation system to simplify the problems. However, sound generation is the main subject of aero-acoustics research; the sound generation mechanism of the musical instrument is especially important for understanding the problem of global instability of vibration. Perceptible sound is the result of the oscillation of vorticity or vertical motion as described by many classical theoretical works by M.S. Howe[3] and other researchers, and is also the result of acoustic coupling among the vibration components, which include the human body, the guide channel, the aperture, and the cylinder of the flute body. It is an aero-elastic instability of the fluid motion problem. Howe's theoretical approach could not clarify the detailed mechanism since there are coupled phenomena. Thus, it is valuable to reinforce the theory with

[1] Cooperative Researcher, Sophia Unviersity,Mechnaical.Eng.,7-1 Kioi-chou Chiyoda-ku Tokyo,102-8554,Japan
[2] Assistant Professor, Arts et Metiers ParisTech,FynFluid,151 bd de l'Hopital,75013 Paris, France

numerical computations. A recent numerical study of the sound generation referring to the shear layer was presented by F. Margnat *et al*.[2] Each role of the terms of Lighthill's equation is carefully evaluated. They contributed to aware the importance of the vorticity and density fluctuation related to both the intensity and propagation direction of sound. And, they illustrated the behavior of the Lighthill source term through a numerical

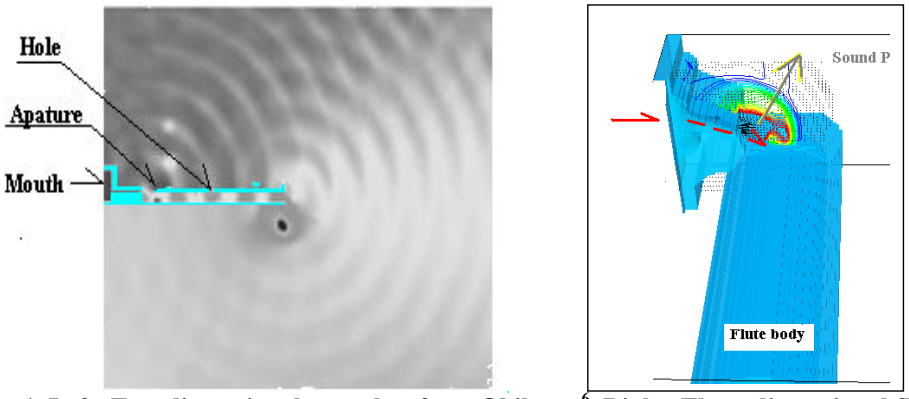

Figure 1. Left: Two dimensional recorder, from Obikane [6]. Right: Three dimensional flute, from Obikane [6].

solution. The Mach number of the mixing layer is higher than the present case but it is related to the motivation of the research.

Successful simulation of the sound generation of the flute family were performed in previous studies [5,6] for two-dimensional recorder, three dimensional recorders, two dimensional flutes, and three dimensional flutes (see Figure 1). These numerical results show aerodynamic differences between recorders and flutes: the flute can easily produce low-frequency tones since it is easy to create stable rotational flow motion in the cylinder. The computations were performed with the compressible Navier Stokes equations. The computations imply that for the low speed sound generation the space of the room (inside the instrument) is essential for creating a stable vortex. i. e. the recorder has rather smaller space in the aperture than the flute. The flute has enough space to create the vortex motion. For the ocarina, the shape is alike the flute and also recorder: it is blown from a side like a flute, but the tone is more like recorder. The computation is made for the ocarina with a guided jet oriented at a 90-degree angle to the cylinder.

In order to interpret the sound power graphically, density gradient correlation distributions are computed for the ocarina configuration and for the mixing layer flow. Indeed, in past works, most interpretations of acoustics waves are not spatial and have examined only frequency and power. One reason is that there is some limitation to do this type of data processing for the massive four-dimensional (time and space) problems. In the present work the morphological interpretation of the patterns were used since aero-acoustic simulations yield complete datasets, which are analyzed. The density gradient correlations (moments) are used as a new spatial variable for representing the acoustic power patterns morphologically with some physical meaning.

The paper is organized as follows: first, the flow configurations are sketched and the numerical method is briefly presented. Then the density gradient correlation method is introduced, before the invariant fields are shown and commented.

II. Flow Configurations and Numerical Aparati

II.A. Ocarina

The geometry for the Ocarina simulation is sketched in Figure 2. The local air speed in the ocarina is about 10m/sec. The compressible Navier Stokes equations can be written as

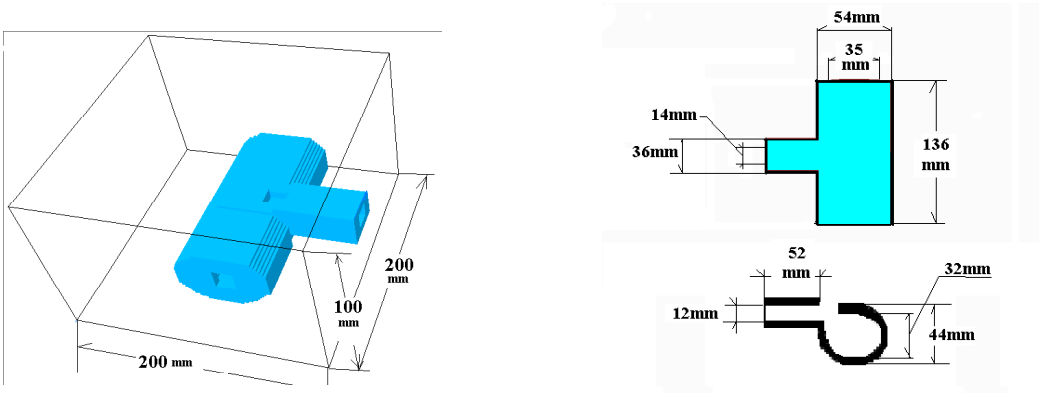

Figure 2. Configuration for the ocarina computation. The air blows from left to right through the channel.

$$\frac{\partial}{\partial t}\left[X_\rho\right]+\begin{bmatrix} \rho u_i \\ \rho u_i u_j + p\delta_{ij} - \tau_{ij} \\ \varepsilon u_i + (p\delta_{ij} - \tau_{ij})\, u_j - \kappa T_{,i} \end{bmatrix}_{,i} = 0 \tag{1}$$

where i=1-3 and j=1-3, Xp= (ρ , ρu_i , ε).

The equation does not include any turbulence model and the viscosity is constant. The computation adds some numerical viscosity. Except in the neighborhood of the ocarina, the problem becomes the acoustic problem.

The explicit scheme is used for time marching with double precision to perform the infinitesimal pressure fluctuations. The cubic mesh size is constant in all directions, so the wave can propagate in the same accuracy. We apply the MUSCL method for the entire domain except boundaries. The boundary conditions at the exits are used unchanged conditions since the flow speed is so slow in the most area. At the outer boundary the method of characteristics condition is necessary to apply to the present case. The frequency and the other characteristics, such as the density gradient correlation were not changed despite of the change of the several boundary conditions. The main frequency was about 3 kHz.

On the wall the speed is set to zero. First, we compute the ocarina of the sides which are open with reflective boundary condition so the acoustic energy is accumulated in the domain and it is easier to see the sound generation. Then the closed ocarina is computed with the no-reflective condition of Poinsot and Lele condition at the one direction.

II.B. Mixing-layer

The compressible Navier-Stokes equations are solved[7] in a computational domain which includes both aerodynamic and acoustic fields of the flow. Such a calculation allows a direct computation of the sound production by the flow, and it allows us to obtain a large database of instantaneous flow quantities, which we can use for the evaluation of the density gradient correlation.

A characteristic-based formulation is used here, in order to facilitate the treatment of boundary conditions. Central sixth-order compact finite differences are used to compute spatial derivatives, while time marching is performed by a fourth-order Runge-Kutta scheme. The code is used to simulate the spatially evolving mixing-layer flow at $Re = \delta_\omega \Delta U/\nu = 400$, where δ_ω is the initial vorticity thickness and $\Delta U = (U_h - U_l)$. The subscripts l and h refer to low and high speed flow, respectively. The initial mean streamwise velocity is given by a hyperbolic-tangent profile, and a small amplitude, incompressible disturbance field is added at the inflow boundary to initiate the transition process. The mixing layer is forced at its most unstable frequencies predicted by the linear theory, in order to control the roll-up and vortex pairing process. A sponge zone is added to dissipate aerodynamic fluctuations before they reach the outflow boundary and to avoid any spurious reflection (see Moser et al.[7] for more details).

The size of the computational domain is L_x = 800 x L_y = 800 which includes a large part of the acoustic field, and the grid resolution is N_x= 2071 x N_y= 785 with a stretched repartition in both directions. The subscripts x and y refer to the streamwise and transverse direction respectively.

In the present paper, two flow regimes are studied: one with M_l=0.25 and M_h=0.5, and the other with M_l=0.4 and M_h=0.8. The associated vorticity and pressure field can be seen in Figure 3. The configuration with the highest Mach number is several times higher than the slowest one, in agreement with classical theory. Moreover, the radiation is more directional: for the fastest configuration, more attenuation is observed upstream (high observation angle), and the maximum radiation direction is sharper.

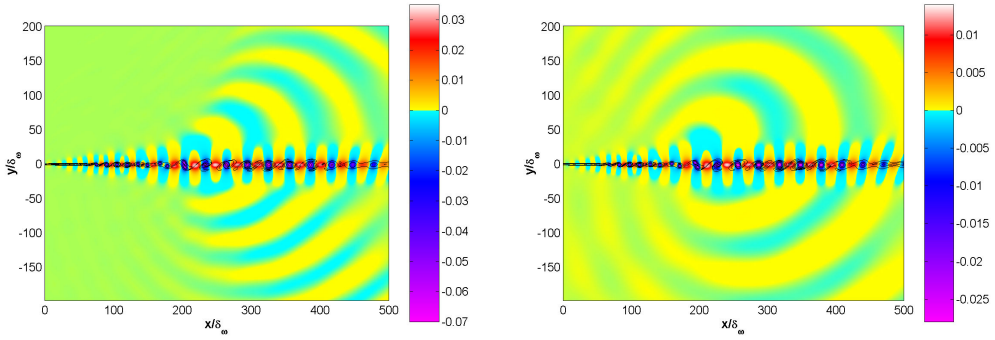

Figure 3. Color plot: instataneous pressure fields of the fluctuating pressure; lines: vorticity contours. Left: M_l=0.25 and M_h=0.5; Right: M_l=0.4 and M_h=0.8.

III. Density Gradient Correlations and its Meaning

III.A. Derivation of the Density Gradient Correlation Equation

In low Mach number flows, it is hard to find the compressibility effects. The infinitesimal compressibility is the sound itself. The infinitesimal disturbance to the mean flow cannot be expressed clearly in usual ways. We assume the Reynolds decomposition, and constitute the correlation of the gradient of the fluctuating density $\rho_{,p}$ which is denoted as $\overline{\rho_{,q}\,\rho_{,k}}$. Here, we should mention that the equation is not the density weighted form for the Reynolds Averaged Navier Stokes equation. The moment equation for the fluctuating density gradient is derived from the continuity equation as follows: (see reference [1])

$$\begin{aligned}\frac{\partial}{\partial t}\overline{\rho_{,q}\rho_{,k}} = -(&\overline{\rho_{,q}u_i}\,\widehat{\rho}_{,jk} + \overline{\rho_{,q}u_{i,k}}\,\widehat{\rho}_{,j} + \overline{\rho_{,q}u_{i,i}}\,\widehat{\rho}_{,k}\\ &+\overline{\rho_{,q}u_{i,ik}}\,\widehat{\rho} + \overline{\rho_{,q}\rho_{,ik}}\,\widehat{u_i} + \overline{\rho_{,q}\rho_{,i}}\,\widehat{u_{i,k}}\\ &+\overline{\rho_{,k}u_i}\,\widehat{\rho}_{,iq} + \overline{\rho_{,k}u_{i,q}}\,\widehat{\rho}_{,i} + \overline{\rho_{,k}u_{i,i}}\,\widehat{\rho}_{,q}\\ &+\overline{\rho_{,k}u_{i,iq}}\,\widehat{\rho} + \overline{\rho_{,k}\rho_{,iq}}\,\widehat{u_i} + \overline{\rho_{,k}\rho_{,i}}\,\widehat{u_{i,k}})\end{aligned} \tag{2}$$

III.B. Two dimensional Case

It is easier to see what is the role of each term in two-dimensional case. For the frozen turbulence approximation in the direction 1, replacing the convection terms with the convective time derivative, then

$$\frac{\partial}{\partial \tau}\overline{\rho_{,1}\rho_{,2}} = -(\overline{\rho_{,1}u_{1,12}} + \overline{\rho_{,1}u_{2,22}} + \overline{\rho_{,2}u_{1,11}} + \overline{\rho_{,2}u_{2,21}})\widehat{\rho}$$
$$-\overline{\rho_{,1}\rho_{,2}}(\widehat{u}_{1,1} + \widehat{u}_{2,2}) - \overline{\rho_{,2}\rho_{,2}}\widehat{u}_{2,1} - \overline{\rho_{,1}\rho_{,1}}\widehat{u}_{1,2} \tag{3}$$

The equation (3) states that the production is done by the mean shear and the mean distortion in the equation, especially the sign of the shear will contribute to the sign of the correlation of the density gradient. i.e. the minus shear direction will give a positive value of the correlation. Here, it should be remarked that there is no explicit viscous effect, the density and velocity correlation reflect the viscosity implicitly.

III.C. Definition of the New Anisotropy Tensors and their Invariant

The equation contains many moments, so anisotropy tensors shown in the moment equation is defined as following. First recall that the anisotropy tensor form *bij*[1] for incompressible flows shown as

$$b_{ij} = \frac{\overline{u_i u_j}}{\overline{u_i u_i}} - \frac{1}{3}\delta_{ij} \tag{4}$$

The fluctuating density gradient is thus defined in a similar way:

$$d_{ij} = \frac{\overline{\rho_{,i}\rho_{,j}}}{\overline{\rho_{,i}\rho_{,i}}} - \frac{1}{3}\delta_{ij} \tag{5}$$

where the isotropy of the tensor d_{ij} takes some values as the wave is one direction as:

$$d_{11} = 2/3$$
$$d_{22} = d_{33} = -1/3 \tag{6}$$

If the second rank tensor is denoted as d_{ij}, then the invariants are expressed as following:

$$\text{The first invariant: } I_d = d_{ii}$$
$$\text{The second invariant: } II_d = (d_{ii}d_{jj} - d_{ii}^2)/2$$
$$\text{The third invariant: } III_d = (d_{ii}d_{jj}d_{kk} - 3d_{ii}d_{jj}^2 + 2d_{ii}^3)/3! \tag{7}$$

IV. Computed Results

IV.A. Ocarina

The discharged flow direction is nearly vertical upward. In that it agrees with the experimental results obtained by K. Ogura in his smoke tunnel of Tamagawa University shown in Figure 4-left. The flow speed was rather higher than the flow speed specified in the computation. The trace (development) of the invariants (II , III) at a point outside of the instrument is shown in Figure 4-right. The invariants are moving from one direction to the other with time in the diagram. We understand qualitatively how the point is distorted by the compression and expansion, also the change of the orientation of the direction of waves before it reaches the steady state as we discuss in section III.

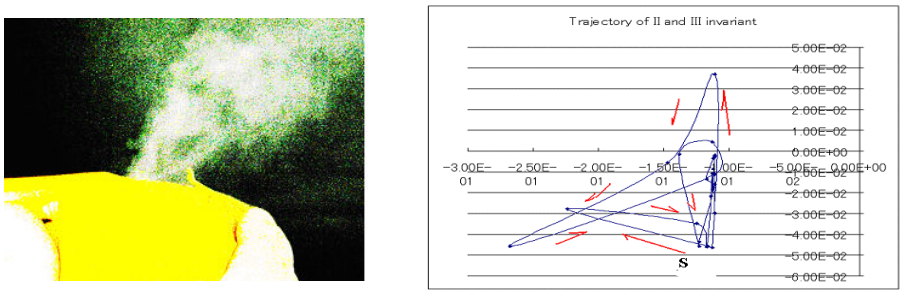

Figure 4. Left: Experimental data shows flow direction is upward to the instrument. Right: Trajectory of (II,III) of a point outside of the Ocarina, The point S indicates the starting point of the trajectories. The movement shows that the point means the histories of the deformation with the strain rates

In the lower resolution images in Figure 5 , we observe the different patterns near the aperture of the instrument. In the higher resolution images in Figure 6 , we can also find the difference between two figures. The blue column from the aperture to the top of the second invariant in Figure 5-left and Figure 6-left can be seen, but there is no remarkable figures in the same locations in the third invariant in Figure 5-right and Figure 6-right. In the same way there are concentric circles near the aperture in the Figure 6-right, but there is no characteristics shape in Figure 6-left. This is a character of the invariants in the principal component analysis. The large bubble areas may be interpreted as the points of node of acoustic waves or source, and the blue line can be seen the directions of the propagation.

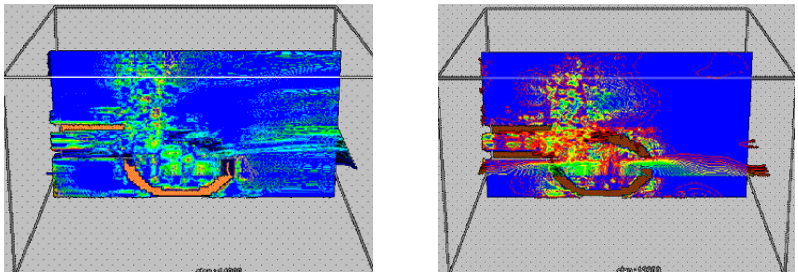

Figure 5. Invariant fields for the Ocarina (coarse mesh 100x60x100). Left: The second invariant. The image shows that the second invariant is not concentrated, but discharged upward from the ocarina. Right: The third invariant. The image shows that the second invariant is concentrated near the aperture of the ocarina

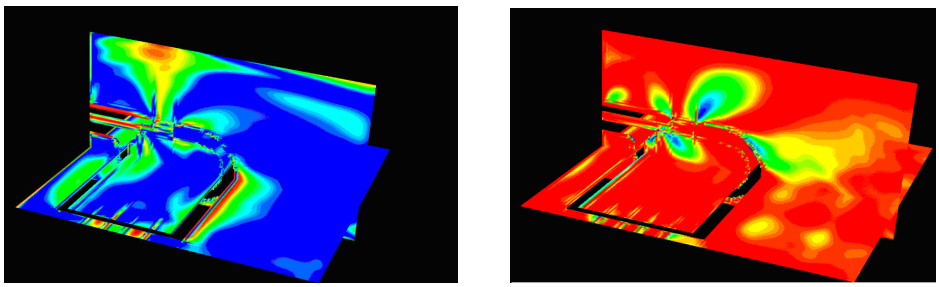

Figure 6. Invariant fields for the Ocarina (finer mesh 200x120x200). Left: The second invariant. The direction of the wave is vertical as the invariant shows. Right: The third invariant. The image is interpreted that there is a source of acoustic energy near the aperture.

IV.B. Mixing-layer

We applied the principal component analysis to make interpretation of the invariant images of Figure 7. There is one black solid line marked A in the left above of Figure 7, and two black lines marked B and C in the right upper Figure 7. These solid lines are not shown in the same position in the lower images. Thus, we can say these are characteristics of the phenomena. With the instantaneous pressure pattern in the left Figure 3, the black line A can be interpreted as the border of the wavy zone and weak-wavy zone, or we may interpret that it is a line of the nodes in angular direction of the spherical wave. As for the higher Mach number of the right images, the pattern is quite similar to one of the lower Mach number, we can see two black lines B and C in different angles which are merged in A. So, we can see the two kinds of waves exist in the results.

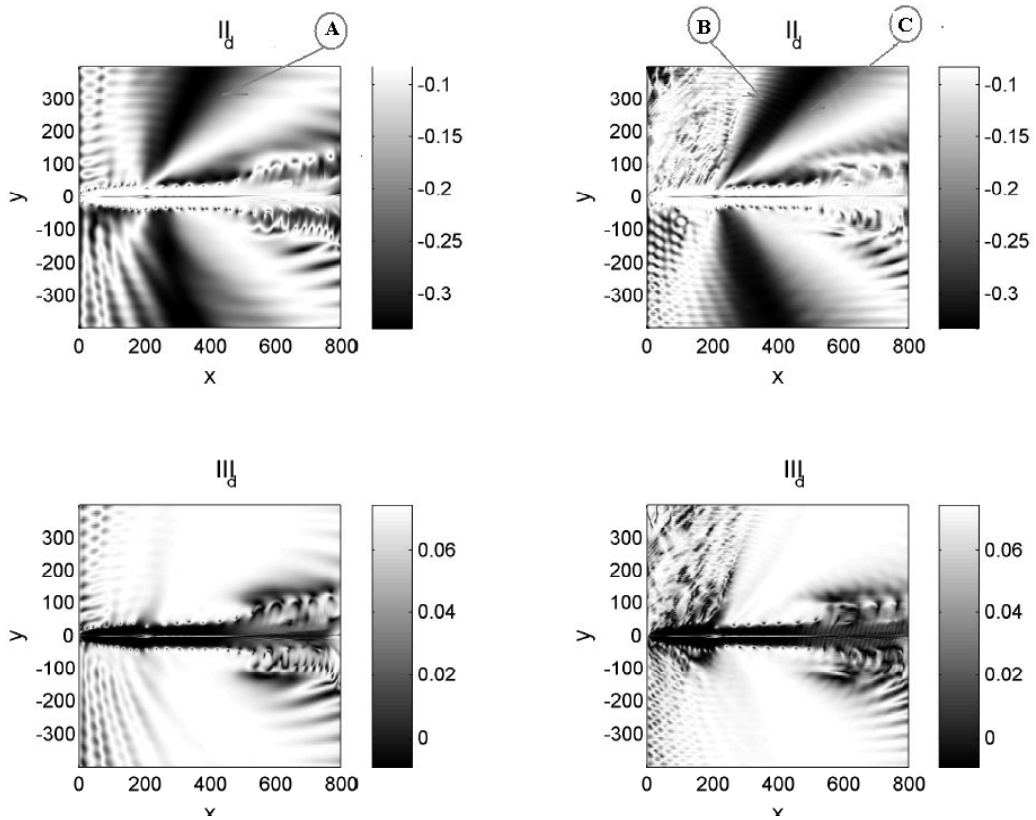

Figure 7. The second invariant and third invariant for mixing-layer. Left: M_l=0.25 and M_h=0.5 , Right: M_l=0.4 and M_h=0.8.

V. Conclusion

The image analysis with the fluctuating density gradient correlation can extract several kinds of signatures that can represent the characteristics of the compressibility: the fluctuating density gradient correlation can represent as the field of the effect of the compression by the mean strain or shear in Ocarina, and also the boundary of the acoustics wave field in the mixing-layer. This illustrates the interest of the method for the analysis of acoustic phenomenon in unsteady subsonic flows.

Acknowledgments

Authors would like to thank Mr. Paul Kunze, graduate student of ENSAM, for calculating the invariants for mixing-layer and tracing the equations, and Arts et Metiers ParisTech where Y. Obikane stayed as an invited professor.

References

[1] Obikane, Y., *Research on the Correlation of the Fluctuating Density Correlation of the compressible Flows*, J. Energy and Power Engineering, Dec.2009,Volume,No.12(Serial No.25) ISSN1934-8975,USA
(WASET, Proceeding, 2009, Dec. TH65000)

[2] Margnat, F., Fortune, V., *An iterative Algorithm for Computing Aeroacoustic Integrals with Application to the Analysis of Free Shear Flow Noise*, J. Acoust. Soc. Am. 128, Issue 4, pp. 1656-1667, 2010.

[3] Howe, M.S., *Contributions to the Theory of Aerodynamics Sound, with Application to excess Jet Noise and the Theory of the Flute*, J.Fluid Mech, vol 71, part 4, pp.625-673, 1975.

[4] Wolfe,L., Smith,J., Tann,J., and Fletcher,N.H., *Acoustic Impedances of Classical and Modern Flutes*, Journal of Sound and Vibration, 243(1), 127-144, 2001.

[5] Obikane ,Y., Kuwahara ,K., *Direct Simulation for Acoustic near Fields Using the Compressible Navier-Stokes Equation*, The Fifth Int. Conf. on Computational Fluid Dynamics, Seoul, South Korea, July 2008.

[6] Obikane, Y., *Direct Simulation on a Fipple Flute Using the Compressible Navier-Stokes Equation*, WASET, ICCFD, Thiland, 2009 DEC. vol60-137 (2009) pp794-798

[7] C. Moser, E. Lamballais, and Y. Gervais, *Direct computation of the sound generated by isothermal and non-isothermal mixing layers*, AIAA Paper 2006-2447 (12th AIAA/CEAS Aeroacoustics Conference), USA, 2006.